TR AE 6708

PLANE-FLAME SIMULATION OF THE WAKE BEHIND AN INTERNALLY PROPELLED VEHICLE

PART 3
EXPERIMENTAL SIMULATION OF A SUPERSONIC VEHICLE BY A DETONATION

by
John H. Skinner, Jr.

This research was supported in part by a NASA Traineeship and in part by the United States Department of Transportation under Contract No. C-117-66 (NEG.).

This paper is taken from part of a thesis to be submitted in partial fulfillment of the requirements for the degree of Doctor of Philosophy in the Department of Aeronautical Engineering and Astronautics at Rensselaer Polytechnic Institute.

DEPARTMENT OF AERONAUTICAL ENGINEERING AND ASTRONAUTICS
RENSSELAER POLYTECHNIC INSTITUTE
TROY, NEW YORK

November, 1967

Acknowledgment

The author wishes to express his appreciation and gratitude to Dr. J. V. Foa for providing advice and guidance throughout the work and to Dr. D. R. White for assistance and suggestions in the experimental phase of the work.

Table of Contents

Abstract

The flow field induced by an internally-propelled vehicle traveling through a tube at a supersonic speed is simulated experimentally by the flow field induced by a detonation. The results indicate that as the vehicle continues to travel at a constant velocity, the effects of friction and heat transfer cause a region of flow to develop which is steady in the frame of reference of the vehicle. This steady-flow region starts directly behind the vehicle and gradually grows to fill the entire flow field as time progresses.

1. Introduction

When analyzing the flow field induced by an internally propelled vehicle traveling at a constant velocity in a tube of infinite length, it would seem logical to treat the flow as steady in the frame of reference of the vehicle. Yet when the vehicle first attains this velocity the flow field may be nonsteady in all frames of reference. Also, attempts to treat the flow as steady[1,2] have met with unexpected difficulties. Therefore a study[3,4] was conducted to determine whether steady-flow actually develops in the vehicle-fixed coordinate system.

In Reference 3 it is shown that for a supersonic vehicle friction and heat transfer cause a steady-flow region to develop gradually from the vehicle rearward, whereas for a subsonic vehicle, as presented in Reference 4, the flow approaches steadiness asymptotically over the entire field. In both of these theoretical analyses a plane flame is used to generate a flow field simulating that induced by an internally propelled vehicle. The purpose of this simulation is to magnify all of the transport rates and dissipative effects that are to be calculated.

In the present paper the flow field induced by a supersonic vehicle is simulated experimentally by that induced by a detonation. The experimental advantages of this simulation are twofold. First it is much easier to produce a constant velocity detonation under laboratory conditions than it is to generate and maintain the required steady supersonic vehicular motion. Secondly, since the dissipative effects are magnified, any trend towards steady flow in the flame-fixed coordinate system should develop much faster and be much easier to detect.

The results of this experimental investigation are compared with the theoretical predictions of Reference 3.

2. Experimental Apparatus

The experimental apparatus is shown schematically on Figure 1.

A 190 ft. length of copper tubing (I.D. 0.527", O.D. 0.625") is sealed at one end by a thin Saran diaphragm. A second diaphragm is placed 75 ft. from the open end. The section of tubing between these two diaphragms is evacuated and then filled with a detonable mixture of hydrogen and air. These gases are well mixed and of uniform concentration throughout the tube. The procedure used to fill the tube and to determine the initial concentrations is described in Appendix 1.

Upon ignition at a point near the center diaphragm a detonation forms and propagates through the mixture, while a retonation shock bursts the center diaphragm and continues to travel through the air towards the open end of the tube. The distance to the open end is made long enough so that reflected waves do not interfere with the flow field during the testing time.

Both the average detonation velocity and the timewise pressure variation resulting after the passage of the detonation are measured at six locations (10 ft. apart) along the tube walls. If the timewise pressure variation is the same at all positions and if the detonation velocity is constant, then the flow is steady in a detonation-fixed coordinate system. Conversely, if the flow is nonsteady, the pressure history varies with position.

Pressure measurements are made with Kistler 603 quartz piezoelectric transducers, whose voltage output is amplified and fed into the vertical deflection system of a Tektronix 535A oscilloscope. The resulting traces are photographed. The pressure is measured at two of the six transducer positions simultaneously. At the four remaining locations the time

of arrival of the detonation is determined by means of piezoelectric ceramics, whose voltage output is used to trigger fast risetime pulse generators. These pulses are fed onto a single trace of the oscilloscope. Knowing the sweep rate of the oscilloscope and the distance between the transducers, the average detonation velocity can be calculated.

Photographs of the detonation tube, filling apparatus, instrumentation, and ignition system can be found on Plates 1 and 2. Photographs of the transducers are presented on Plates 3 and 4, while detailed information about the instrumentation system can be found in Appendix 2.

3. Experimental Results

The experimental results for a detonation propagating into a mixture of 30% hydrogen and 70% air ($2.04\ H_2 + O_2 + 3.76\ N_2$) at 70° and atmospheric pressure, are presented on Plates 5 - 7.

The oscilloscope sweep is triggered when the detonation reaches transducer position 1. Plate 5 shows the pressure history after the passage of the detonation at positions 1 and 6, 50 and 100 ft. from ignition respectively. Plate 6 is the pressure history at positions 2 and 4, 60 and 80 ft. from ignition, while Plate 7 shows the pressure history at positions 3 and 5, 70 and 90 ft. from ignition. On each of the oscillograms a trace showing the pulses produced when the detonation arrives at the remaining transducer locations is also shown. A small arrow in the right hand margin of the oscillogram indicates the zero pressure level in cases where it is not immediately apparent on the traces.

The detonation velocity in the test region is constant to within $\pm$ 60 ft/sec at 6210 ft/sec. This is within the accuracy of the velocity measuring system as described in Appendix 2B.

As the detonation passes the pressure transducers, the sudden impact causes ringing of the quartz crystals. This is especially apparent at positions 3 and 5. The crystal vibration was found to be dependent upon both the mounting of the transducer and the support of the detonation tube at the transducer location. As the crystal vibrations damp out it can be observed that the resulting pressure history is the same at all locations for approximately 5 msec. after the passage of the detonation. Therefore in this region the flow field is steady in a detonation-fixed coordinate system.

On each of the pressure traces there are small variations which perturbate the smooth pressure decay. Similar to the crystal vibrations, these perturbations were found to be dependent upon the local nonuniformities in the mounting and support of the detonation tube. However these variations do not alter the overall pressure history (except in their immediate vicinity) and therefore can be ignored.

On Plate 5 the pressure jump at position 6 after about 8 msec. is due to the shock reflected from the end diaphragm. Therefore the pressure history at this location should be compared to the others only up to the arrival of this shock.

The ringing of the crystals immediately after the passage of the detonation was observed in more detail on faster oscilloscope sweeps. The detailed structure of the vibration is shown for position 2 on Plates 8 and 9. At a sweep rate of 10 μsec/cm (Plate 9c) a large initial overshoot in crystal output can be observed. This overshoot is followed by an undershoot which actually goes below the zero pressure level. After this however the crystal does damp down to a more regular vibration pattern. The centerline of this vibration is shown as a dotted curve on Figure 2. Figure 2a corresponds to Plate 8c while Figure 2b corresponds to Plate 9b. The upper and lower curves on these figures are the locus of vibration maxima and minima respectively. It can be seen that the centerline can be extrapolated back to an initial pressure level of approximately 195 psi. This is of the same magnitude as the pressure predicted by the Chapman-Jouguet theory (for a mixture $2H_2 + O_2 + 3N_2$ the C-J pressure is 197 psi).

A comparison between the experimental results and the theoretical predictions for the detonation studied in the previous analyis is shown on Plates 10 - 13. Part (a) of these plates shows the pressure

history at various locations as predicted by the analysis for inviscid adiabatic flow. (See Appendix 3a). In this instance the flow field is nonsteady in a detonation-fixed coordinate system. This is apparent by the difference in pressure at various locations at corresponding times after the passage of the detonation (Table 1).

Part (b) of these plates shows the pressure history predicted when friction and heat transfer are accounted for. (See Appendix 3B). In this case the flow field is steady and the pressure histories are identical. Also the initial pressure gradient immediately behind the detonation is found to be very much greater when friction and heat transfer are accounted for.

Part (c) shows the experimental results. As has been previously noted the flow field is steady in a detonation-fixed coordinate system.

The experimental pressure variation is qualitatively similar to that given by the theoretical analysis including friction and heat transfer as the rate of pressure variation immediately after the detonation passes is initially very steep but then levels off as time progresses. However the actual pressure does decrease faster than as predicted by the theoretical analysis. For example the rate of pressure change .2 msec. after the detonation passes is approximately 115 psi/msec., while the analysis predicts a rate of 98.5 psi/msec. Also 3 msec. after the detonation has passed the pressure has dropped to 40 psi while the theoretical pressure is 65 psi.*

---

* In making quantitative comparisons it should be remembered that the theoretical analysis and experimentation were performed for slightly different mixtures. The detonation velocities differ by about 2% while the peak pressures differ by about 9%.

Figure 3 shows the pressure at various transducer locations plotted as a function of distance from the detonation front (Appendix 3B). From this figure it can be seen that there is a growing region where the flow is steady in a detonation-fixed coordinate system. The theoretical steady flow pressure distribution in a reference frame moving with the detonation is also shown in this figure.

The experimental results indicate that dissipative effects in the flow field induced by a detonation are actually greater than those assumed in the analysis. At any point a fixed distance from the detonation front, the observed pressure slope is generally steeper than theoretically predicted and the corresponding pressure level is therefore lower.

In the analysis the friction factor C_f is assumed constant throughout the entire wake region and the heat transfer coefficient is related to the friction factor using the Reynolds' analogy. Actually, the friction factor varies inversely with the Reynolds number and, as the flow velocity decreases, C_f increases. Also, since the Reynolds analogy is only valid for turbulent flow it does not properly account for heat transfer in low Reynolds number regions. Condensation of water vapor in the products of combustion also alters the heat transfer rate and causes a decrease in observed pressure.

Differences between theoretical and experimental results in the immediate vicinity of the detonation are probably due to neglection of real gas effects in this region. Also it should be noted that the experimental results immediately behind the detonation are somewhat obscured by transducer vibrations.

Although the results of the theoretical analysis do not agree quantitatively with the experimental observations, they do provide a valid

qualitative description of the pressure history (an initially very steep pressure slope and subsequent leveling off as time progresses). More important however, is the fact that the simplified theoretical model accurately predicts the development of a region of steady flow in the detonation-fixed coordinate system.

Plate 14 presents the pressure history at various locations along the tube for a rich mixture of 40% H_2 and 60% Air. As before the pressure histories are the same for a growing region behind the detonation, and in this region the flow field is steady.

4. Conclusions

Since the flow field induced by a detonation is qualitatively similar to that induced by a supersonic internally propelled vehicle, the results of this experimental study apply qualitatively to both situations. Therefore, when a vehicle travels at a constant velocity in a tube of great length, friction and heat transfer cause a growing region of steady flow to develop in the vehicle-fixed coordinate system. The experimentally observed development of steady flow is correctly predicted by the previous theoretical analysis although the latter underestimates the magnitude of the dissipative effects.

5. APPENDICES

Appendix 1. Filling Procedure and Determination of Initial Concentrations

In order to provide thorough mixing of the detonable gases the tube is filled simultaneously at the same location with hydrogen and air.

The molar flow rates of the two gases are maintained constant during filling, thereby insuring a uniform mixture throughout the tube. This is accomplished by using critical flow needle valves in the filling lines upstream of the gas inlets. The gas delivery pressures are kept high enough so that sonic flow exists in the throats of the needle valves and the resulting molar flow rates are therefore constant.

The needle valves are calibrated in the following manner. The tube is evacuated, the hydrogen delivery pressure is set at a prescribed value, and the hydrogen needle valve is opened to a specified throat size. As the tube fills with hydrogen the timewise pressure variation is recorded. When the pressure in the tube reaches atmospheric, the flow of hydrogen is stopped, and the filling time is noted. This procedure is then repeated for the compressed air.

The timewise pressure variation is checked for linearity for each gas in order to verify constant molar flow rates. The tube is then filled simultaneously with both gases. The ratio of the number of moles of hydrogen to the number of moles of air in the gaseous mixture (F) is equal to the air filling time divided by the hydrogen filling time. The percentages by volume of each of the gases are:

$$\%\, H_2 = \left(\frac{F}{1+F}\right) \times 100\% \quad , \quad \%\, AIR = \left(\frac{1}{1+F}\right) \times 100\%$$

where

$$F = m_{H_2} / m_{AIR} .$$

Appendix 2. Instrumentation

A. Pressure Measuring System

The pressure history behind the detonation is measured with Kistler 603A quartz piezoelectric transducers. These transducers are shock mounted in brass bosses (Plate 3a) which are in turn mounted on the tube (Plate 3b). The transducers are exposed to the flow field through a small orifice in the tube wall.

These transducers have the following specifications [6]

Pressure range	to 3000 psi
Resolution	.5 psi
Resonant Frequency	400 KC
Risetime	1 μ sec
Insulation resistance	10^{13} ohms
Flash Temperature Range	to 3000^{o}F
Nominal sensitivity	0.35 picocoulomb/psi
Capacitance	20 picofarads

The transducer output is amplified by a Kistler 504 charge amplifier. These amplifiers have the following specifications [7]

Input impedance	10^{9}, 10^{11}, 10^{14} ohms
Output voltage	$\pm$ 10 volts
Frequency response	DC to 100 KC
Input capacitor	10 to 50,000 picofarads

An important consideration in making piezoelectric measurements is the decay constant of the transducer amplifier system. [8] The response of such a system to a step pressure p is a negative exponential

$$V = \frac{G\,p\,k}{C}\, e^{-t/t_d}$$

where V is the voltage output of the system, C is the input capacitance, G is the gain of the amplifier, and k is the crystal sensitivity. The time decay constant t_d is the product of the input capacitance and the input resistance of the system. It is important to have a very large decay constant so that the response decays very slowly as time progresses. Since increasing the input capacitance of the system results in a decrease in the magnitude of the voltage output, the decay constant must be kept large by establishing a very high input resistance. For an input resistance of 10^{11} ohms and an input capacitance of 100 picofarads the time constant is t_d = 10 secs. Therefore for the time intervals considered in the experiment (t max $\approx$ 15 msecs), $e^{-t/t_d} \approx 1.0$ and $V \approx \frac{GPk}{C}$.

By increasing the input resistance of the amplifier to 10^{14} ohms the time constant becomes 10,000 seconds (the magnitude of the response is unchanged) and static calibration of the system is possible.

The system was statically calibrated using a dead weight tester in the following manner.

The gain of the amplifier (G) is set equal to 1/k, while the input capacitor is set equal to 100 picofarads. Therefore the sensitivity of the system is .01 volts/psi. Various pressures are applied to the transducer using the dead weight tester and the output voltages are viewed on the oscilloscope. The resulting calibration curves are shown on Figure 4. The transducer sensitivity of transducer #S/N1238 was determined to be .360 picocoulombs/psi. The face of transducer #S/N1237 was slightly damaged during mounting and the sensitivity decreased to .285 picocoulombs/psi.

The amplifier gain was verified using standard amplitude calibration voltages and the frequency response was verified up to 50 KC.

The vertical deflection of the oscilloscope can be read to an accuracy of ± 0.0125 volts at .5 volts/cm. Therefore pressure measurements made with this system are accurate to ± 1.25 psi.

B. Detonation Velocity Measuring System

The arrival time of the detonation at various positions along the tube is measured with lead-zirconate-titanate (PZT) piezoelectric ceramic discs (1/4" diameter, 1/10" thick, piezoelectric modulus of 2.5 $\frac{\text{volts/in}}{\text{psi}}$). These discs are mounted in a manner similar to the pressure crystals (Plate 4).

When the detonation passes, these transducers produce a voltage output which is used to trigger a fast risetime pulse generator (risetime determined to be less than 1μ sec.) The pulses are fed into a single trace of the oscilloscope. The risetime of the oscilloscope is approximately 25 nanosec.

The average detonation velocity between any two transducers is determined in the following manner.

The distance between the centers of the piezoelectric discs is measured to an accuracy of 1/16". Since the disc diameter is 1/4" the total inaccuracy between any two transducers is 5/16". The distances between the transducers positions are:

From position 1 to position 2 ---- 9' 11-3/4" ± 5/16"

From position 2 to position 3 ----10' 1/4" ± 5/16"

From position 3 to position 4 ---- 9' 10-1/4" ± 5/16"

From position 4 to position 5 ----10' 1-1/2" ± 5/16"

From position 5 to position 6 ---- 9' 11-3/4" ± 5/16"

The total inaccuracy in the passage time of the detonation

between any two transducer positions is the sum of the risetimes of the pulse generators and the oscilloscope plus the inaccuracy in reading the oscilloscope trace. The inaccuracy in reading the oscilloscope trace is determined to be $\pm$ .025 msec at a sweep rate of 1 msec/cm. Therefore the total inaccuracy in time measurement is $\pm$ .026 msec.

The average detonation velocity is:

$$u_D = \frac{\Delta x}{\Delta t} = \frac{\overline{\Delta x} + \varepsilon_x}{\overline{\Delta t} + \varepsilon_t}$$

$\overline{\Delta x}$ is the nominal distance between any two transducers

$\overline{\Delta t}$ is the time between any two pulses on the oscilloscope trace

ε_t and ε_x are the inaccuracy in time and distance measurements respectively.

$$u_D \simeq \frac{\overline{\Delta x}}{\overline{\Delta t}} \left(1 + \varepsilon_x/\overline{\Delta x} + \varepsilon_t/\overline{\Delta t}\right)$$

For $\overline{\Delta x}$ = 10 ft, $\varepsilon_x = \pm$ 5/16", $\varepsilon_t = \pm$ .25 msec and $\overline{\Delta t}$ = 1.60 msec.

$$u_D = 6250\,(1 \pm .019)\ \text{f/s}.$$

Therefore the velocity measurements are accurate to approximately $\pm$ 2%.

Appendix 3. Theoretical Pressure Histories

A. Pressure Histories for Inviscid Adiabatic Flow

The pressure histories at the transducer positions along the tube wall, for inviscid adiabatic flow, are obtained from the pressure distributions in a detonation-fixed coordinate system in the following manner.

The nondimensional detonation velocity is $U_D = 4.919$. For a speed of sound in the detonable mixture of $a_o = 1240$ f/s, the detonation velocity is $U_D = 6100$ f/s. It is assumed that the detonation starts impulsively at the center diaphragm and travels at this constant velocity for the length of the tube.

In order to use the theoretical pressure distribution curves of L_o must be chosen so that τ and ξ are within the range plotted (except for this consideration the value of L_o is completely arbitrary for inviscid adiabatic flow). L_o is chosen as 4.0 ft.

The pressure at any position x along the tube wall at time t is determined in the following manner.

Calculate $X = x/L_o$, $\tau = t a_o / L_o$, and $X_D = \frac{U_D t}{L_o} = \tau U_D$

Then $\xi = X_D - X$

The pressure distribution curves are entered with the calculated value of τ and ξ and the pressure is recorded. This is repeated for various values of time at each of the transducer locations and the corresponding pressure histories are obtained.

B. Pressure Histories for Flow with Friction and Heat Transfer

The pressure histories for flow with friction and heat transfer are obtained in a similar manner to those for inviscid and adiabatic flow.

The major difference is that in the present case L_o cannot be chosen arbitrarily.

All of the state variables on the right hand side of the characteristic equations are multiplied by the factor $C_f L_o / r$. Therefore the pressure distribution for flow with friction and heat transfer depends upon the physical properties of the tube as well as the state of the gas. In the theoretical analysis C_f = 0.01, r = 2 in., and L_o was chosen as 5.280 ft. Therefore $C_f L_o / r$ = .3168. In order to use the theoretical pressure distribution to predict the pressure history for the experimental tube (C_f = 0.003, r = 1/2 in) L_o must be chosen as 2.2 ft. so that $C_f L_o / r$ remains the same.

6. References

1. Foa, J.V., "Propulsion of a Vehicle in a Tube," Rensselaer Polytechnic Institute, TR AE 6404, Troy, New York, June 1964.

2. Hagerup, H.J., "A Note on the Flow Induced by a Disturbance Traveling in a Tube," Rensselaer Polytechnic Institute, TR AE 6405, Troy, New York, June 1964.

3. Skinner, J.H., Jr., "Plane Flame Simulation of the Wake Behind an Internally Propelled Vehicle -- Part 1 - Simulation of A Supersonic Vehicle by a Detonation," Rensselaer Polytechnic Institute, TR AE 6701, Troy, New York, March 1967.

4. Skinner, J.H., Jr., "Plane Flame Simulation of the Wake Behind an Internally Propelled Vehicle -- Part 2 - Simulation of a Subsonic Vehicle by a Heat Source," Rensselaer Polytechnic Institute, TR AE 6705, Troy, New York, July 1967.

5. Lewis, B. and Von Elbe, G. Combustion Flames and Explosions of Gases, Academic Press, New York 1961.

6. Operating and Service Instructions - Kistler Quartz Pressure Transducers Model 603A, H and L. The Kistler Instrument Corporation, Clarence, N.Y., 1966.

7. Operating and Service Instructions - Model 504 Universal Dial-Gain Charge Amplifier. The Kistler Instrument Corporation, Clarence, N.Y., 1966.

8. Arons, A.B., and Cole, R.H., "Design and Use of Piezoelectric Gauges for Measurement of Large Transient Pressures," The Review of Scientific Instruments, 21, January 1950, p. 31.

TABLE 1

Pressure at various locations at corresponding times after the passage of the deontation. (Inviscid Adiabatic Flow)

	Position	Time after passage of detonation	
1	50 ft from ignition	2 msec	137.5 psi
		5	87.5
2	60 ft from ignition	2	145
		5	97.5
3	70 ft from ignition	2	152.5
		5	107.5
4	80 ft from ignition	2	157.5
		5	115
5	90 ft from ignition	2	162.5
		5	-
6	100 ft from ignition	2	167.5
		5	132.5

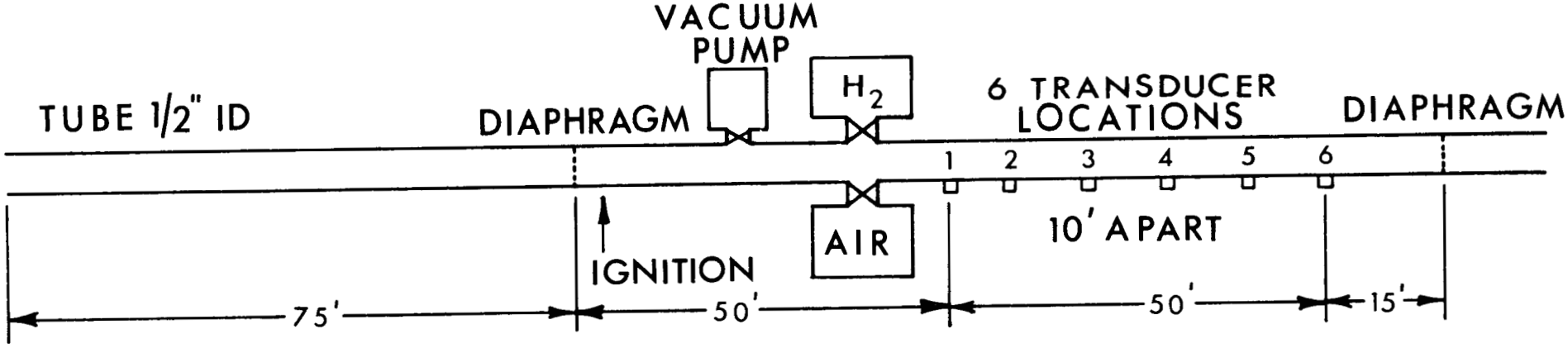

FIGURE 1 Schematic of the experimental apparatus

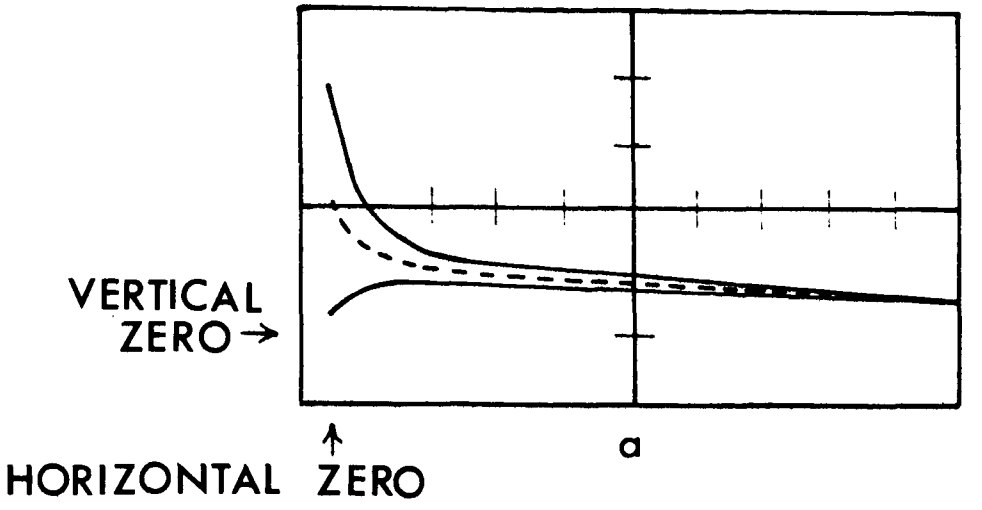

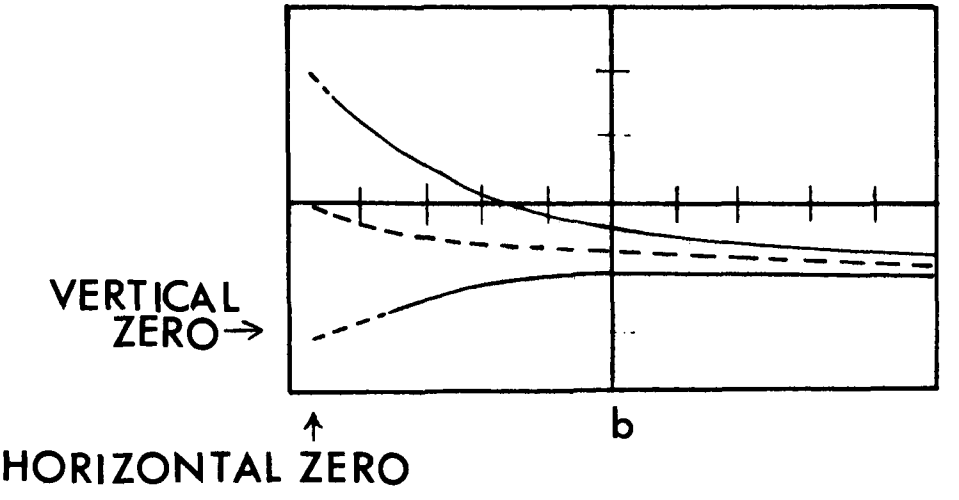

FIGURE 2 Centerline of pressure transducer vibration pattern at position 2. (Upper curve is locus of vibration maxima, lower curve is locus of vibration minima, middle curve is centerline).

a. vertical 100 psi/cm, horizontal .1 msec/cm
b. vertical 100 psi/cm, horizontal 20 μ sec/cm

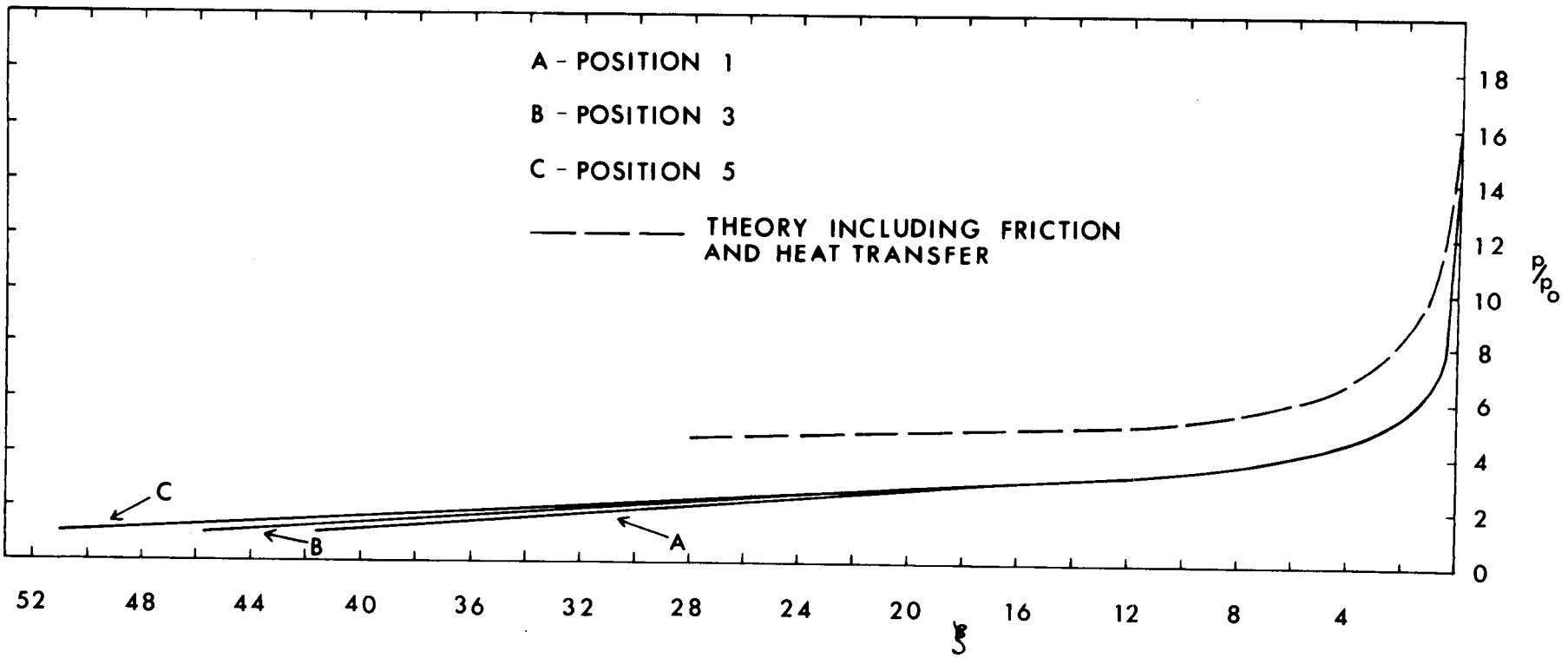

FIGURE 3 Pressure at various transducer locations in a coordinate system fixed to the detonation. (ξ is nondimensional distance from the detonation front).

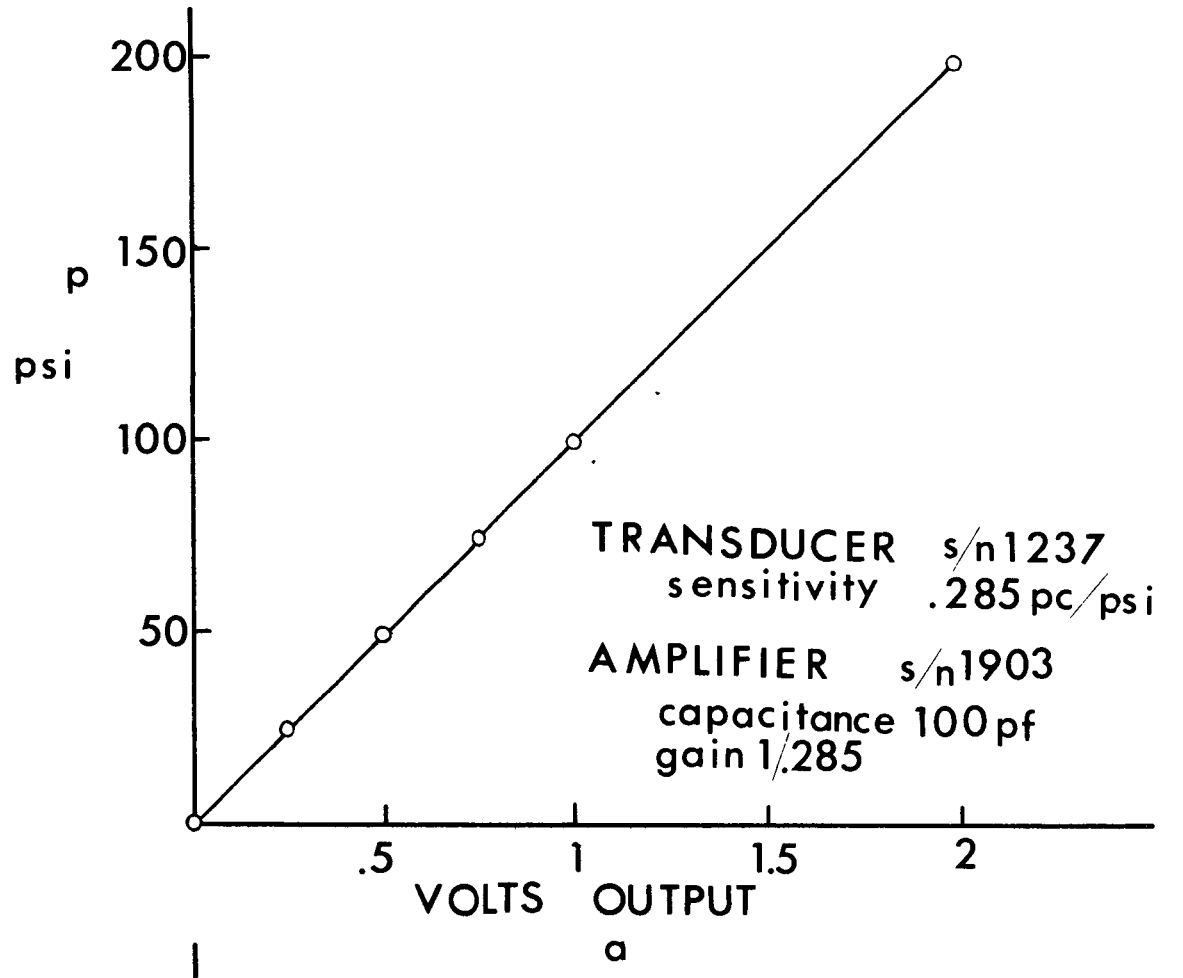

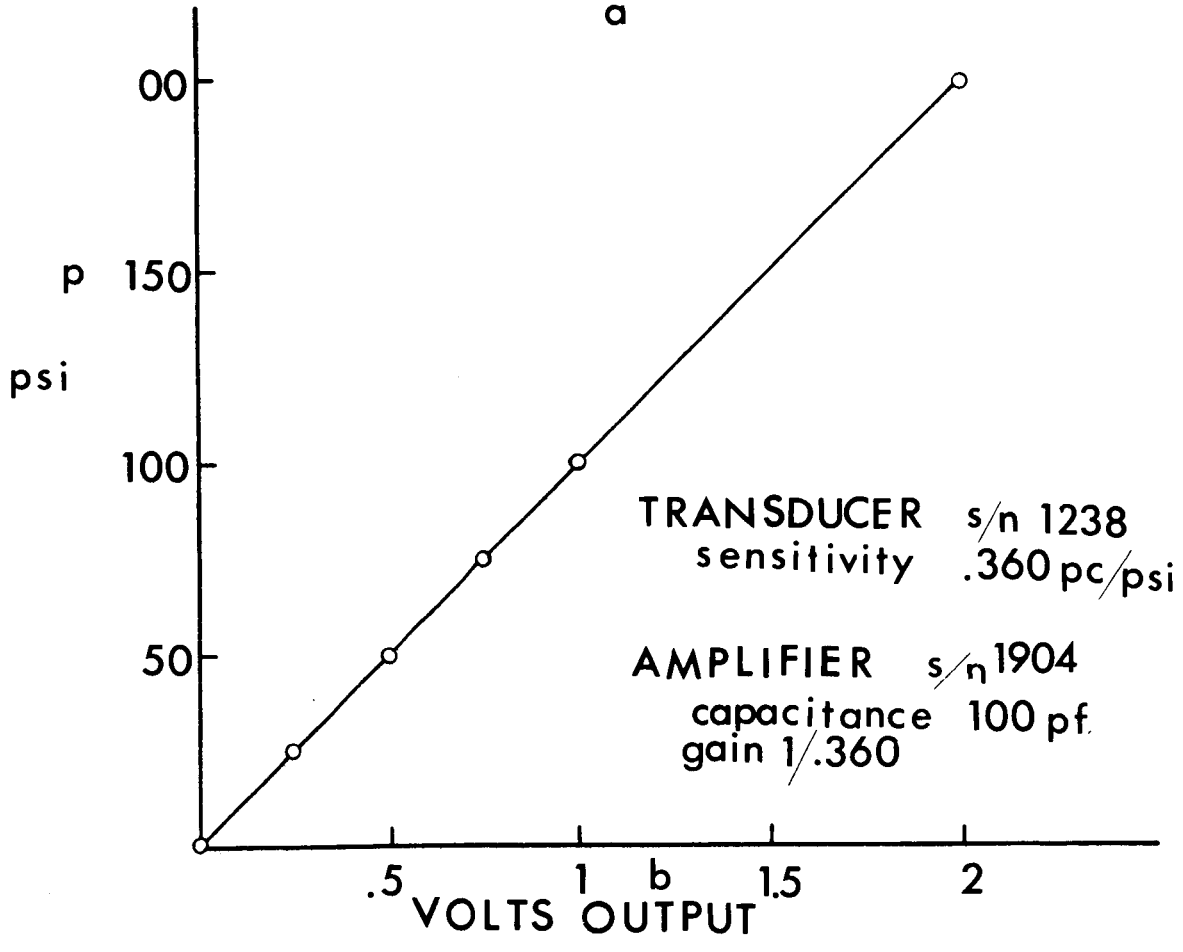

FIGURE 4 Calbiration curves for pressure transducer-amplifier system

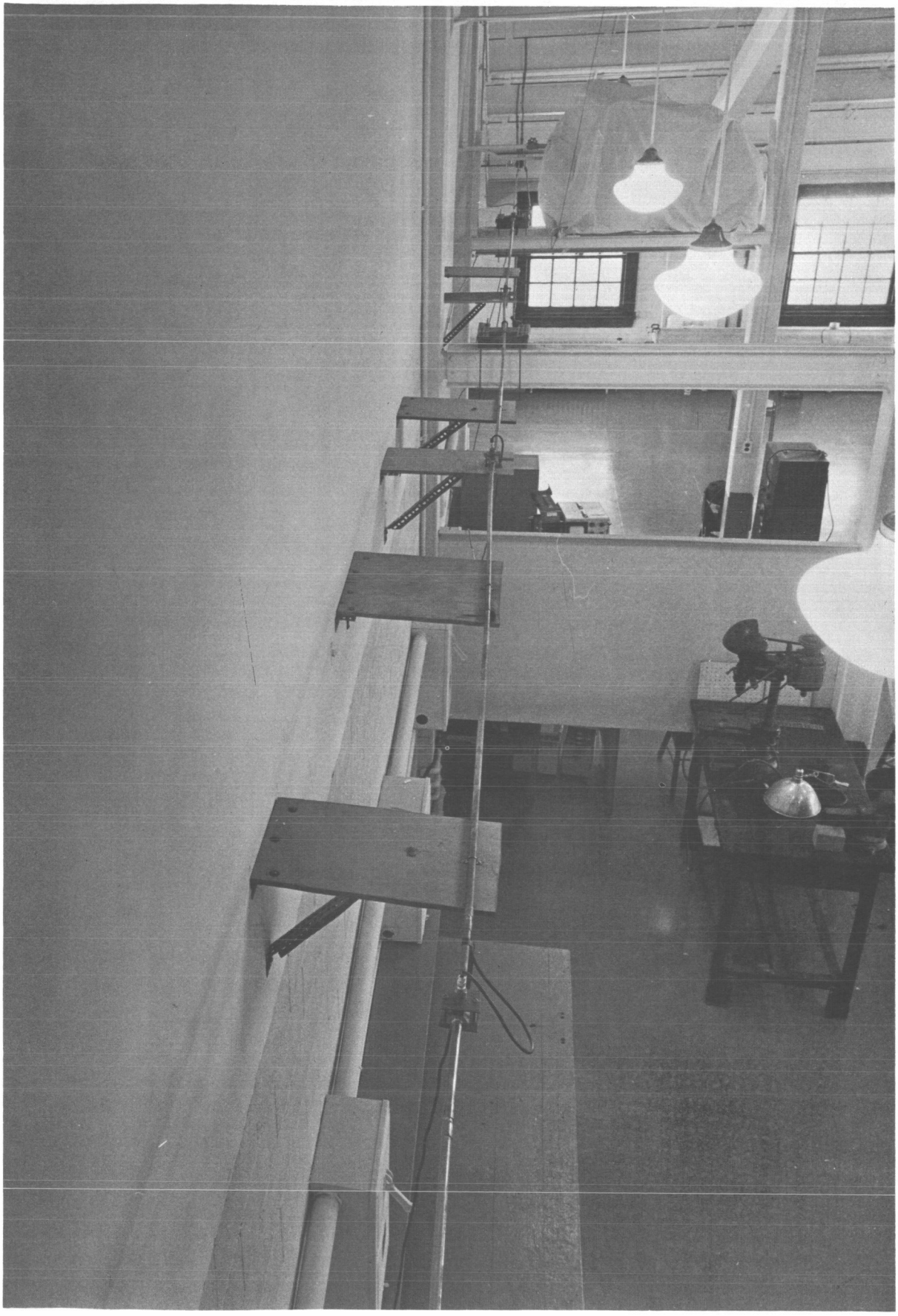

PLATE 1 Test section of detonation tube facing the closed end. Transducer position 3 is visible in foreground.

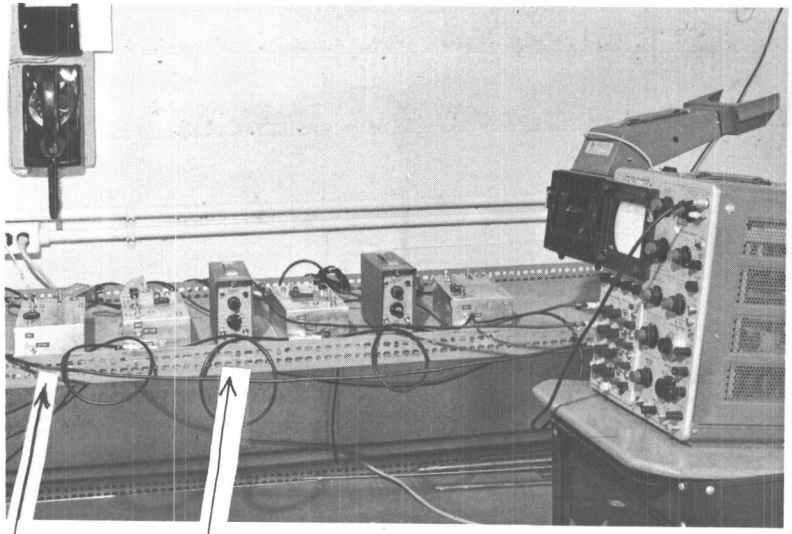

a

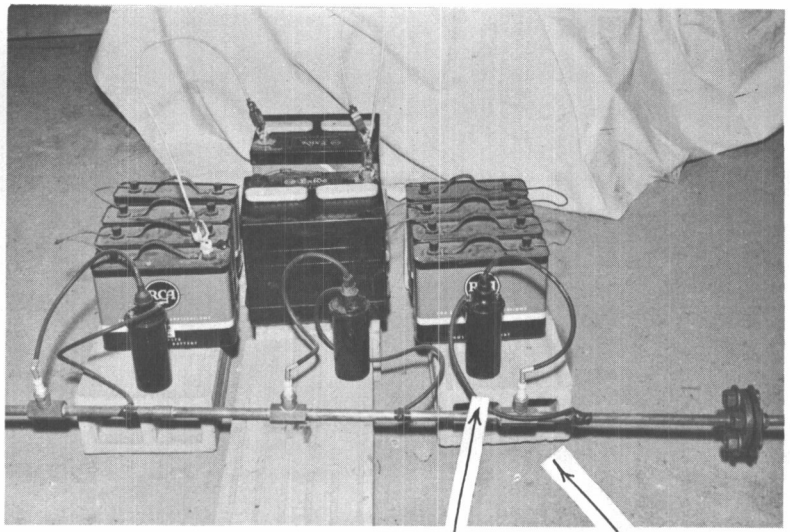

b

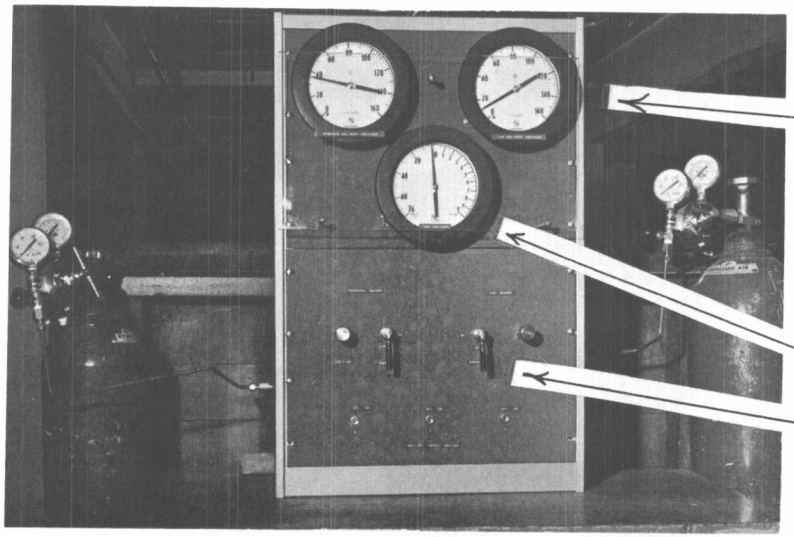

c

PLATE 2
a. Instrumentation
b. Ignition system. (Center diaphragm is mounted in flange at right
c. Filling system

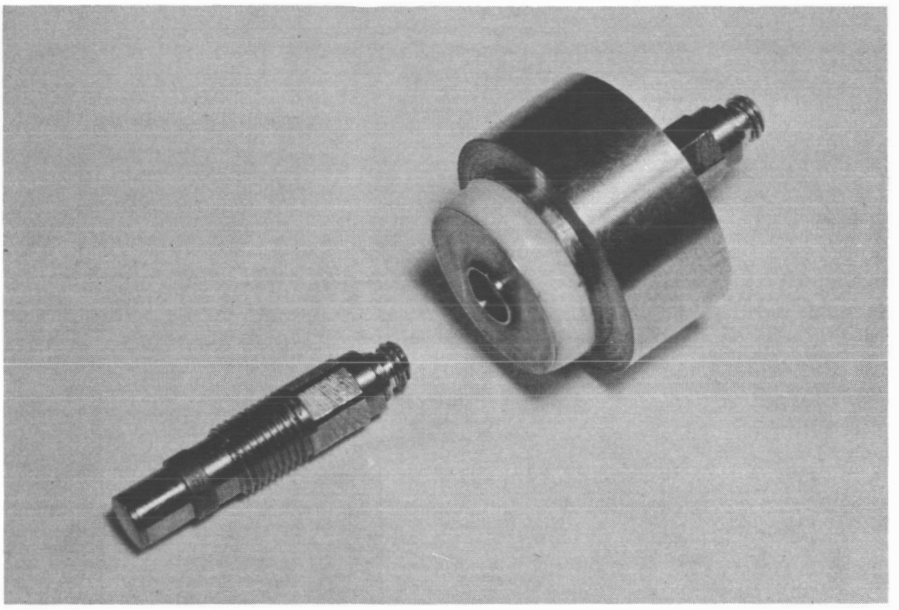

a

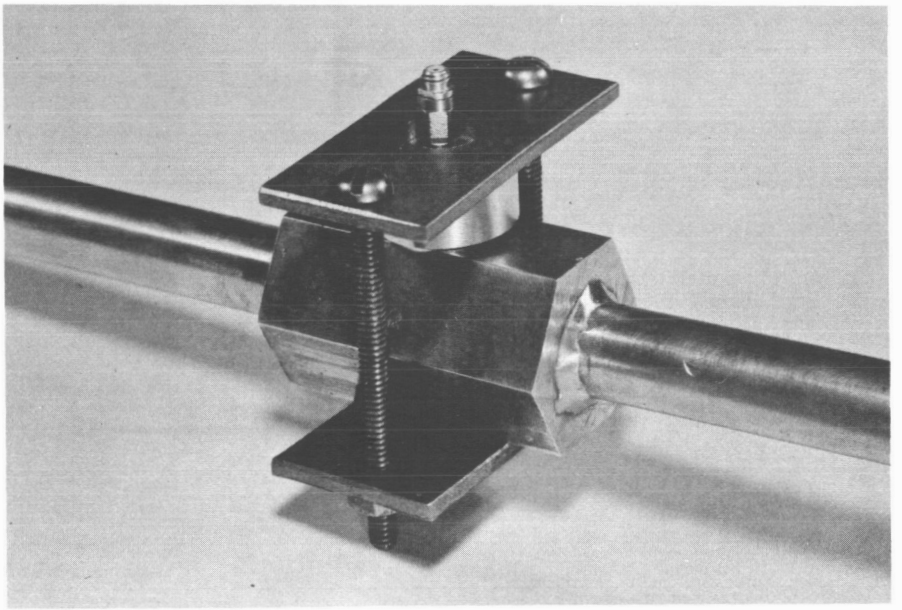

b

PLATE 3 Pressure Transducer

a. Kistler 603A transducer mounted in brass boss.
b. Pressure transducer assembly mounted on detonation tube

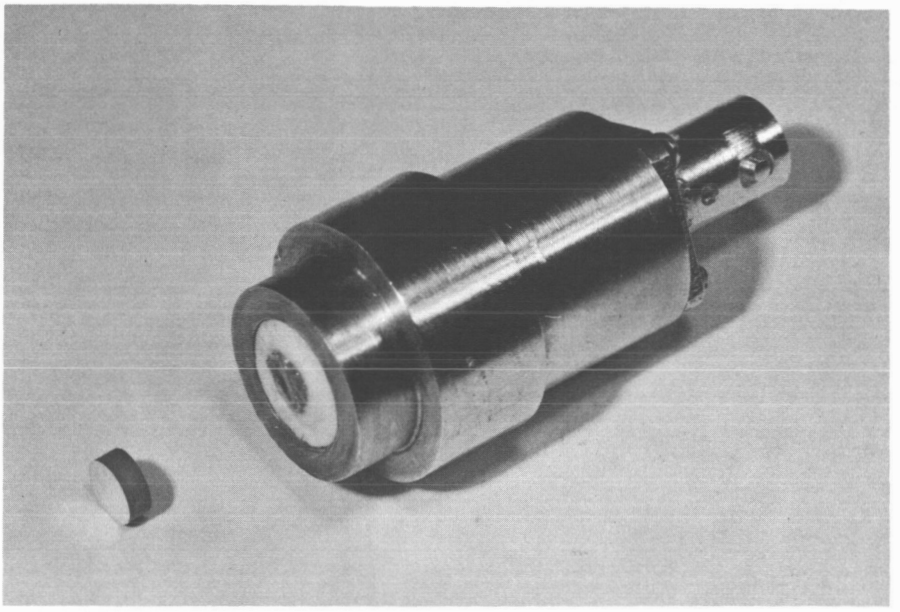

a

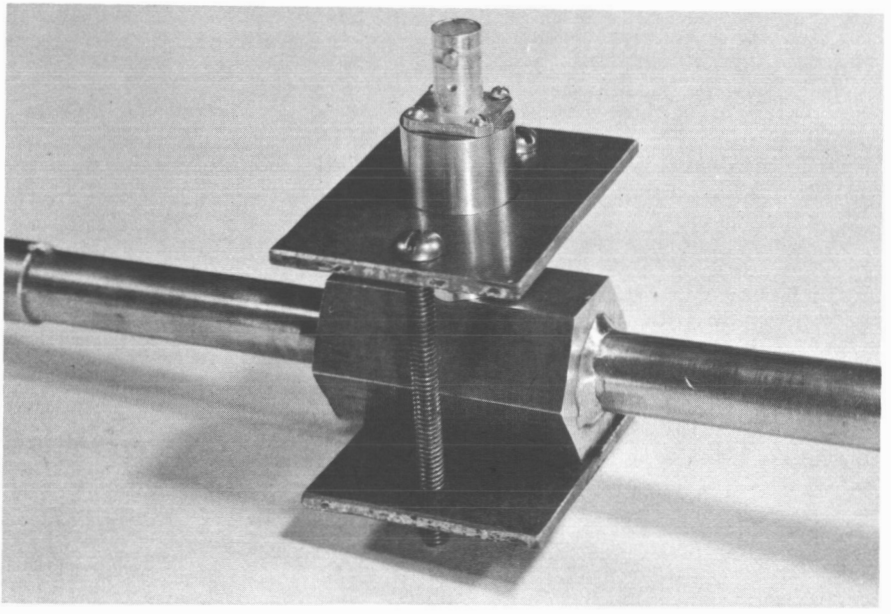

b

PLATE 4 Time of Arrival Transducer

a. PZT ceramic disc mounted in brass boss
b. Time of arrival transducer assembly mounted on detonation tube.

a

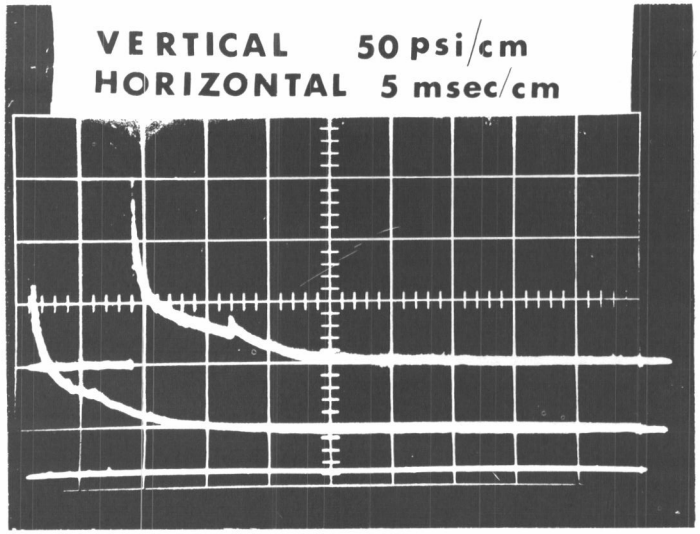

b

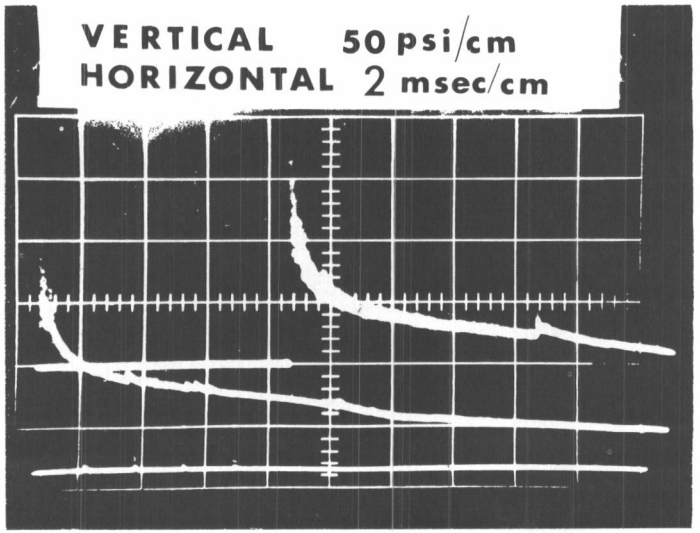

c

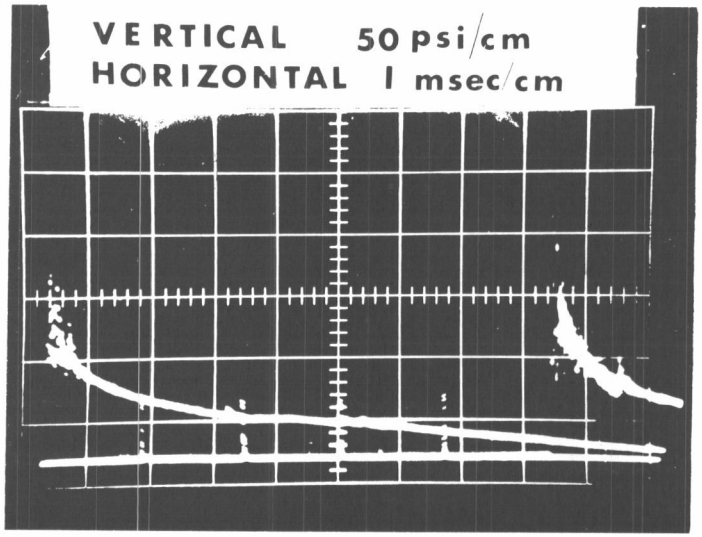

d

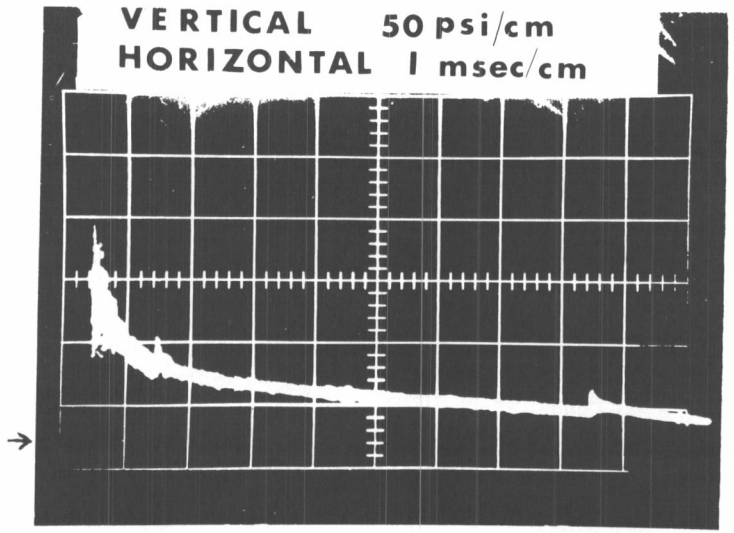

PLATE 5 Pressure history at positions 1 and 6, 50 and 100 ft. from ignition respectively. (Mixture: 30% H_2, 70% Air, at 70°F and 1 atm.)

a

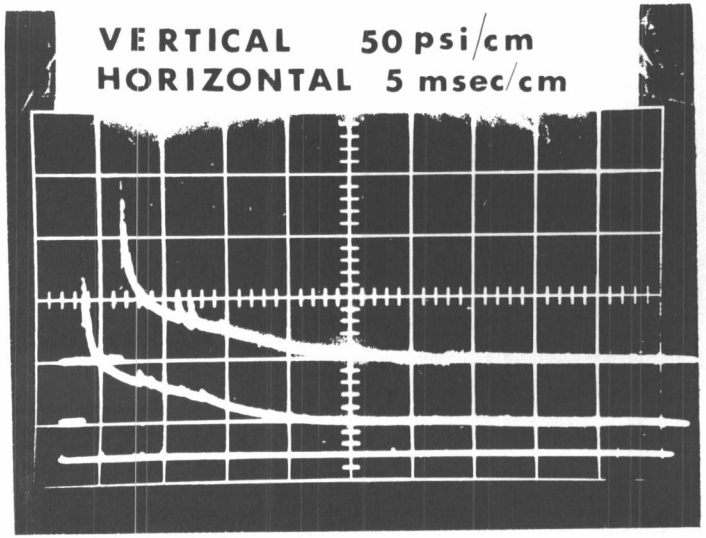

b

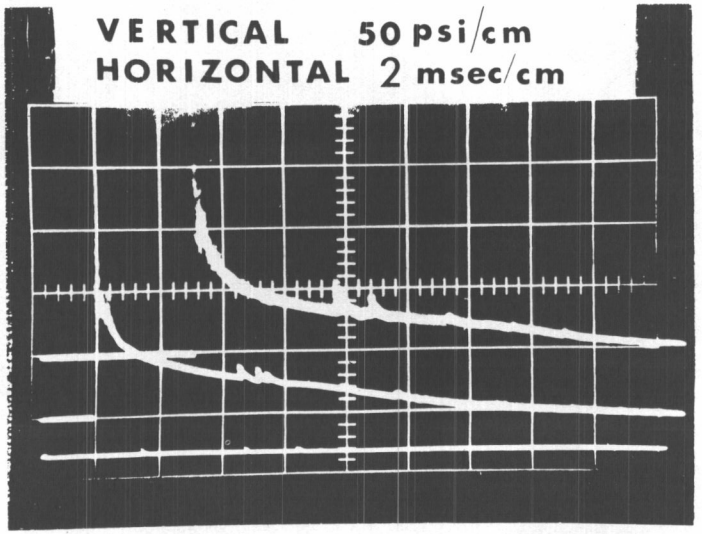

c

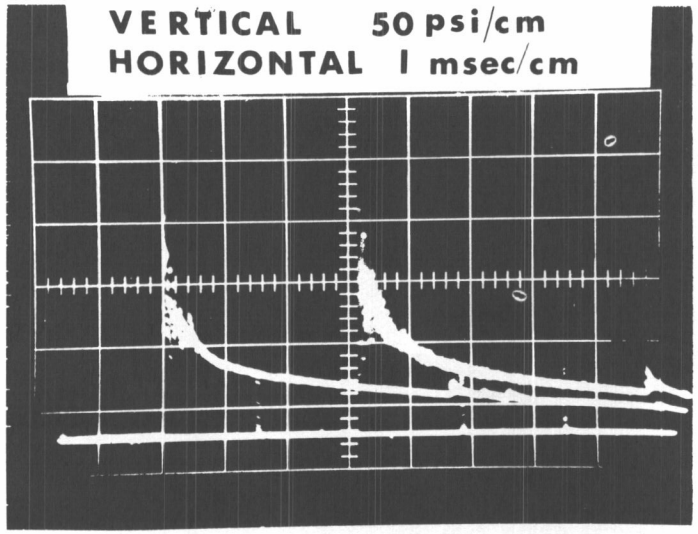

PLATE 6 Pressure history at positions 2 and 4, 60 and 80 ft. from ignition respectively. (Mixture: 30% H_2, 70% Air, at $70^{o}F$ and 1 atm.)

a

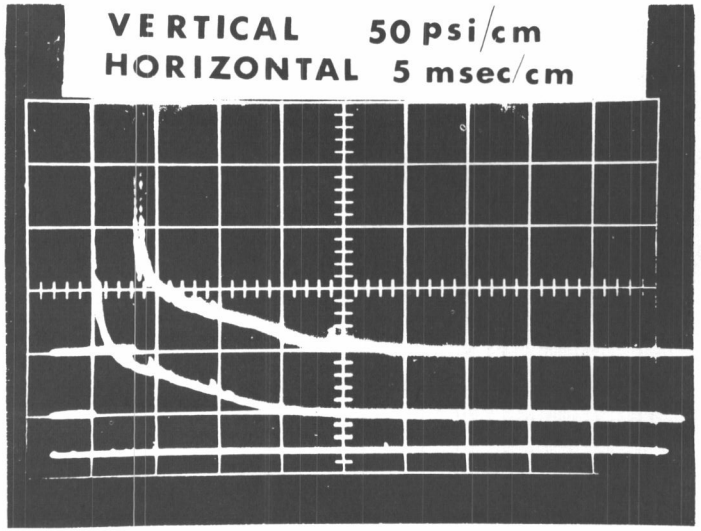

b

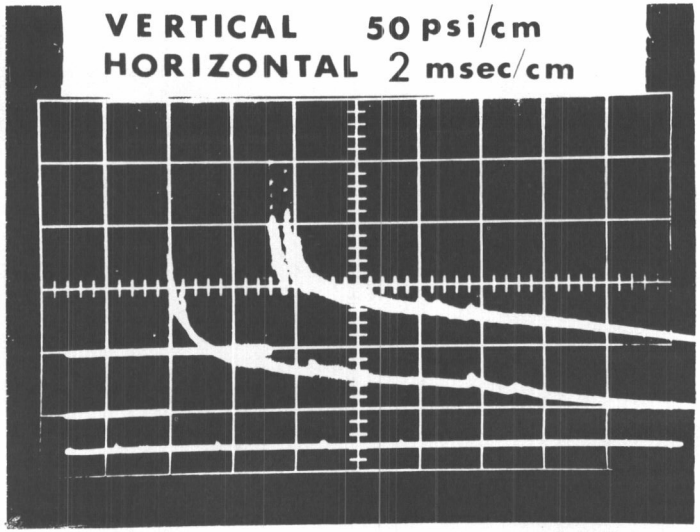

c

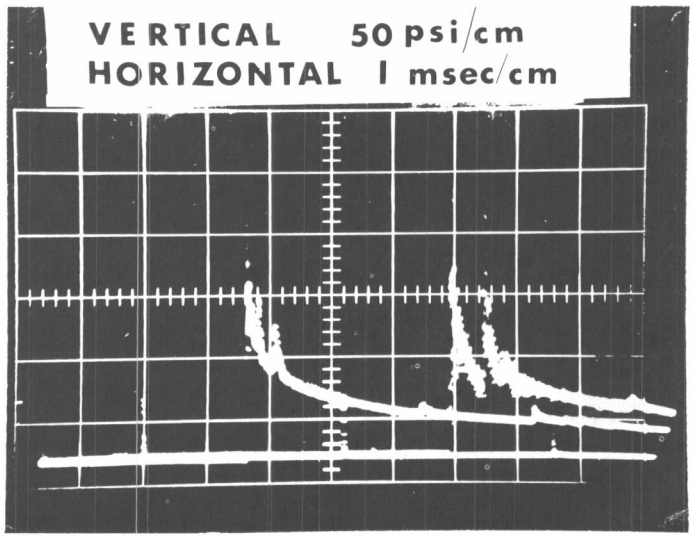

d

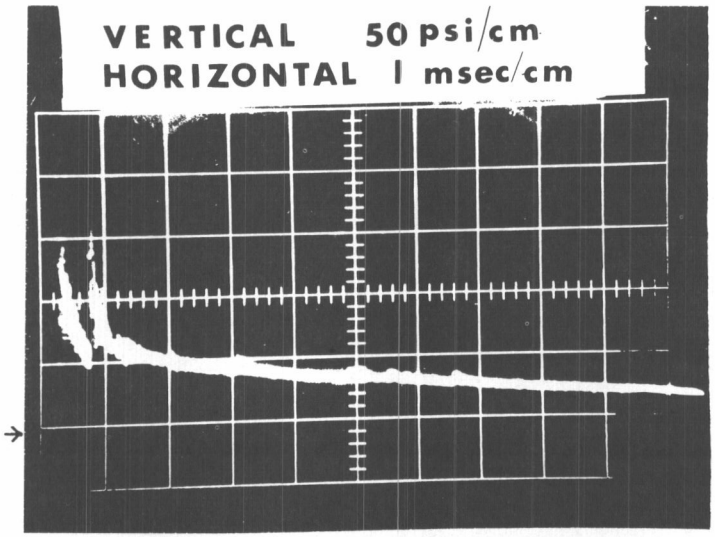

PLATE 7 Pressure history at positions 3 and 5, 70 and 90 ft. from ignition respectively. (Mixture: 30% H_2, 70% Air, at 70°F and 1 atm.)

a

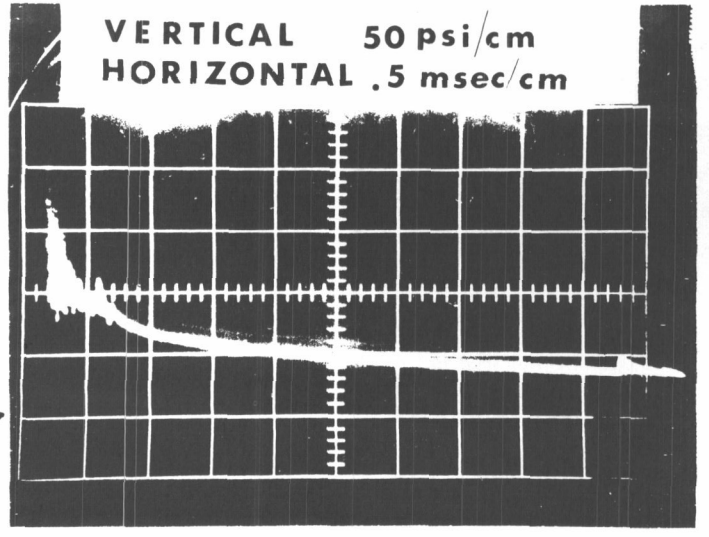

b

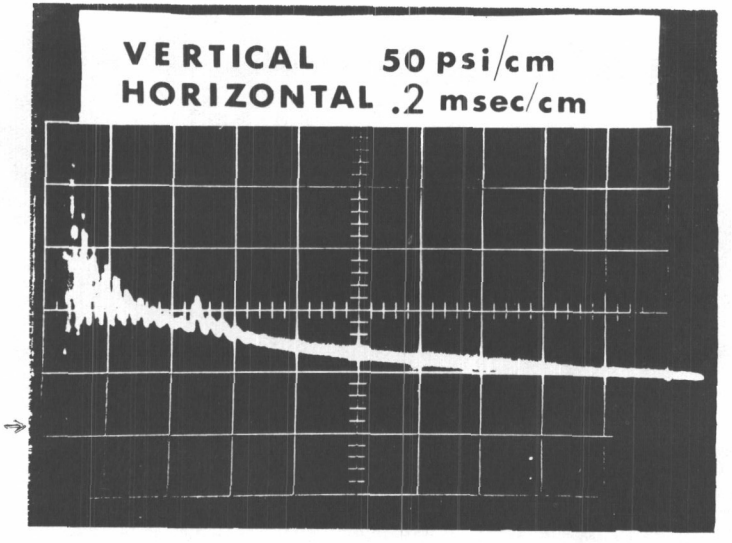

c

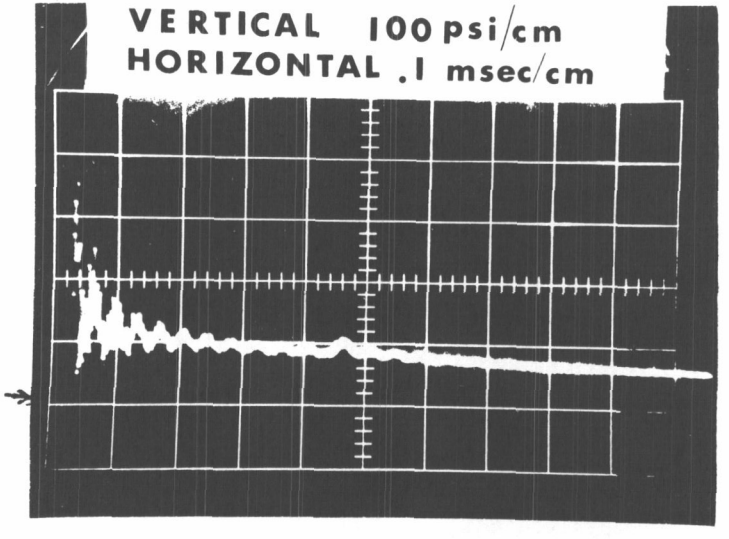

PLATE 8 Pressure history at position 2 observed at fast sweep rates. (Mixture: 30% H_2, 70% Air at 70°F and 1 atm.)

a

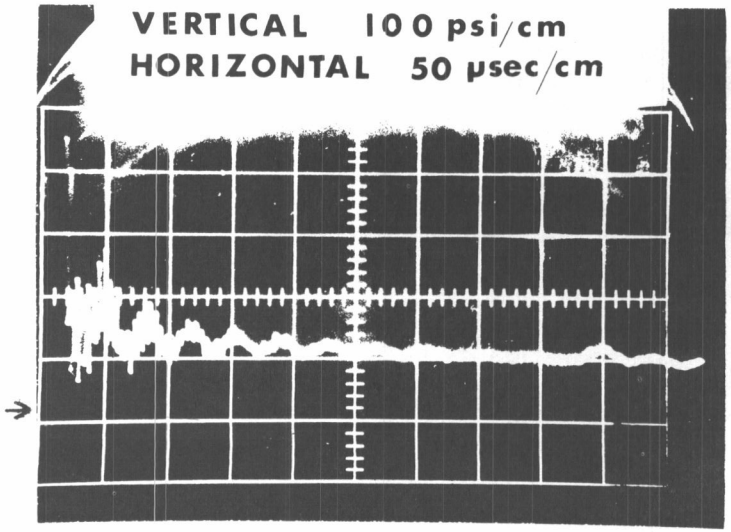

b

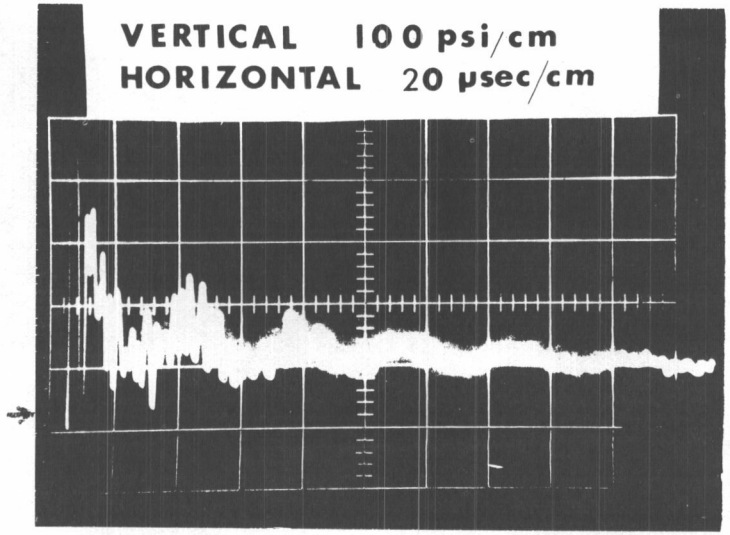

c

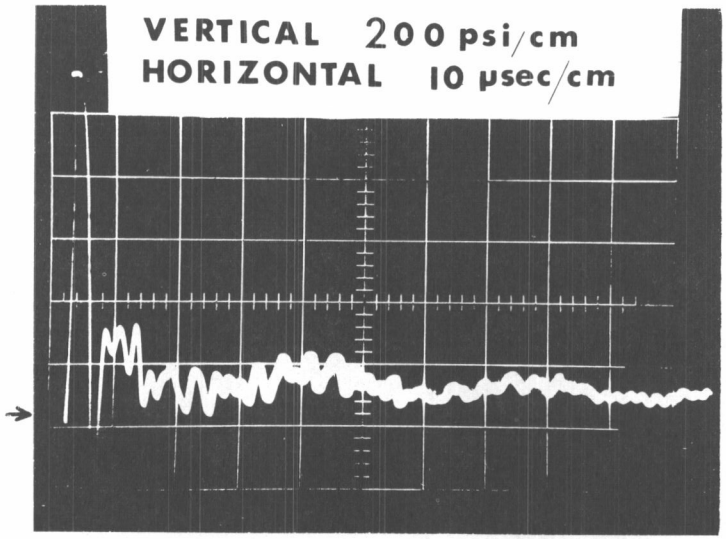

PLATE 9 Pressure history at position 2 observed at fast sweep rates (continued)

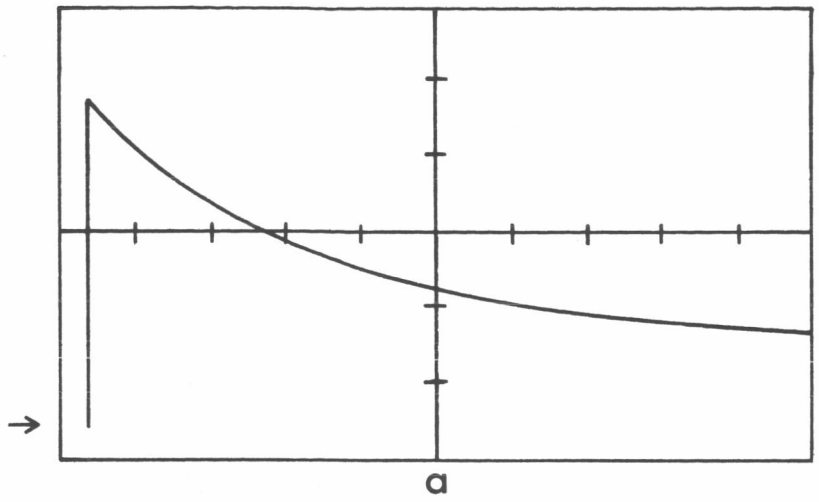

a

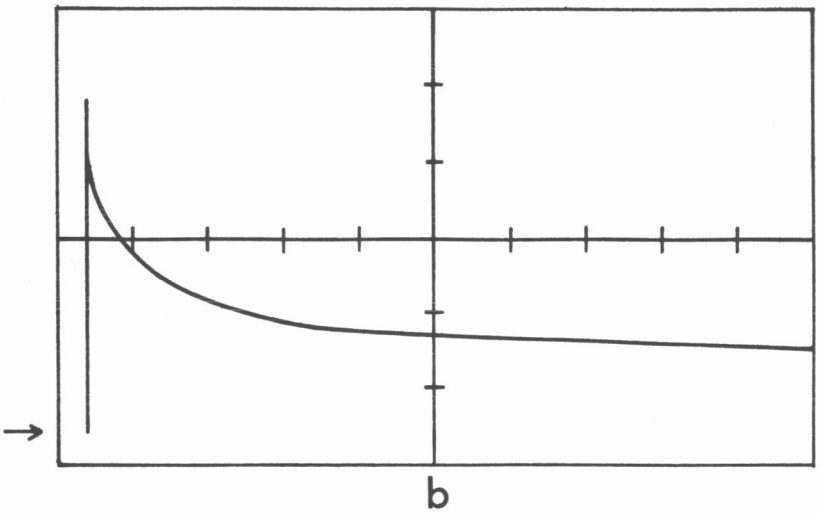

b

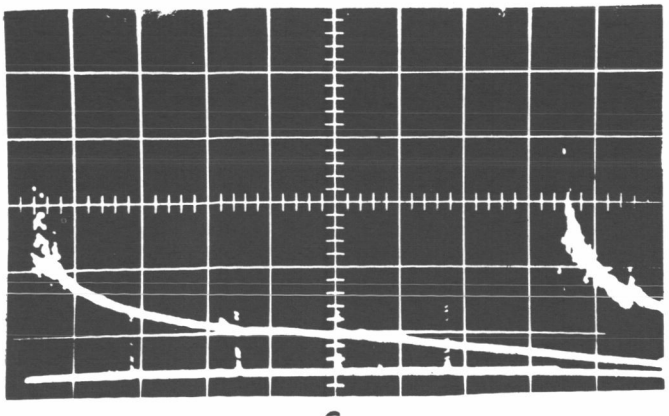

c

PLATE 10 Comparison of theoretical and experimental pressure histories.
(Position 1, vertical 50 psi/cm, horizontal 1 msec/cm)

a. Theory for inviscid and adiabatic flow
b. Theory including friction and heat transfer
c. Experimental result

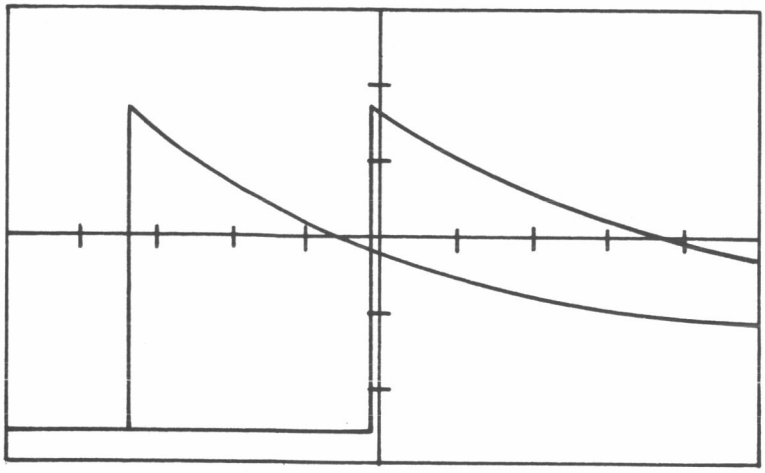

a

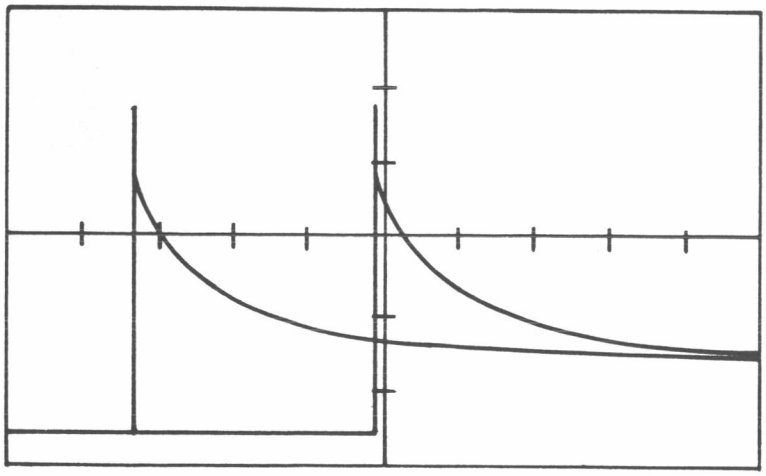

b

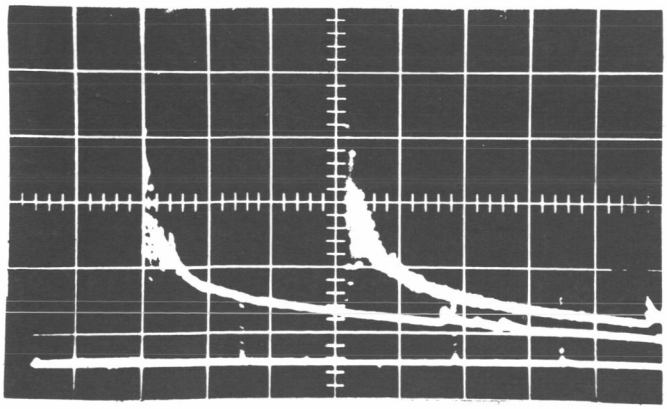

c

PLATE 11 Comparison of theoretical and experimental pressure histories (Positions 2 and 4, vertical 50 psi/cm, horizontal 1 msec/cm)

a. Theory for inviscid and adiabatic flow
b. Theory including friction and heat transfer
c. Experimental result

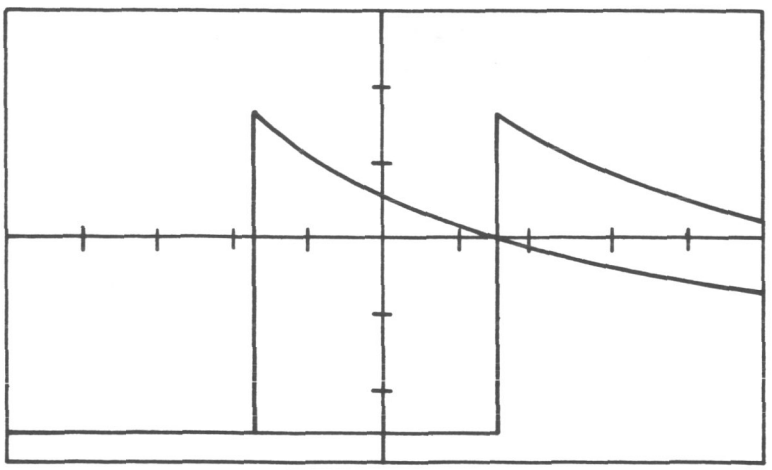

a

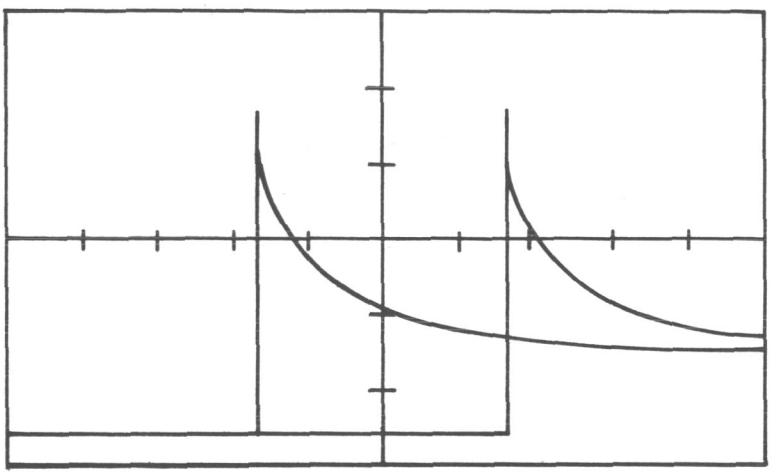

b

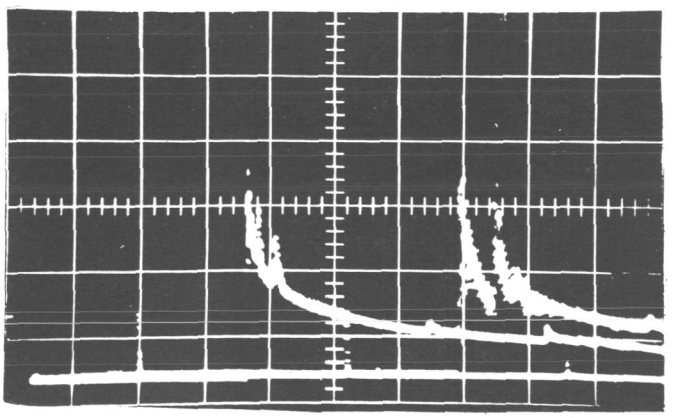

c

PLATE 12 Comparison of theoretical and experimental pressure histories (Positions 3 and 5, vertical 50 psi/cm, horizontal 1 msec/cm)

a. Theory for inviscid and adiabatic flow
b. Theory including friction and heat transfer
c. Experimental result

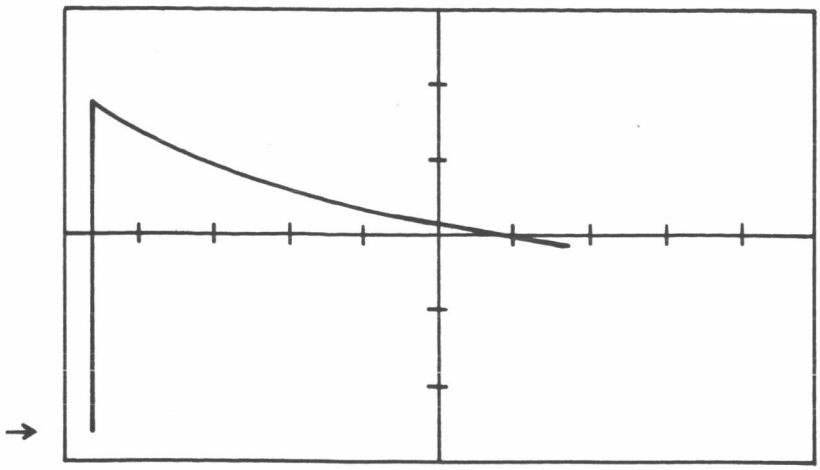

a

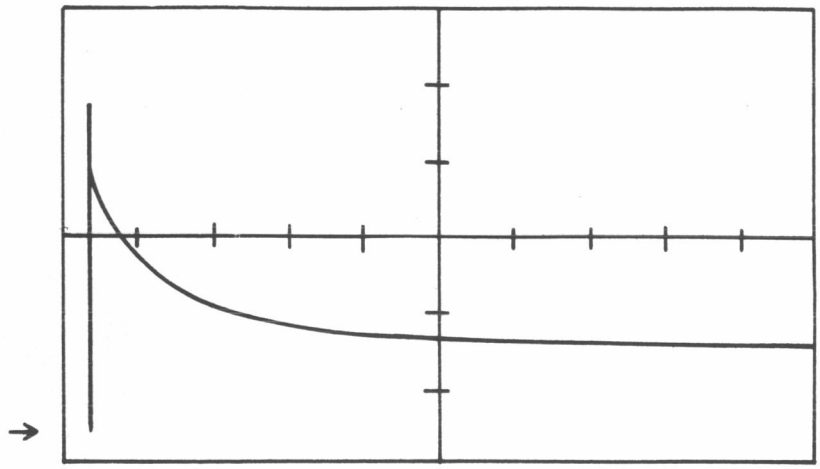

b

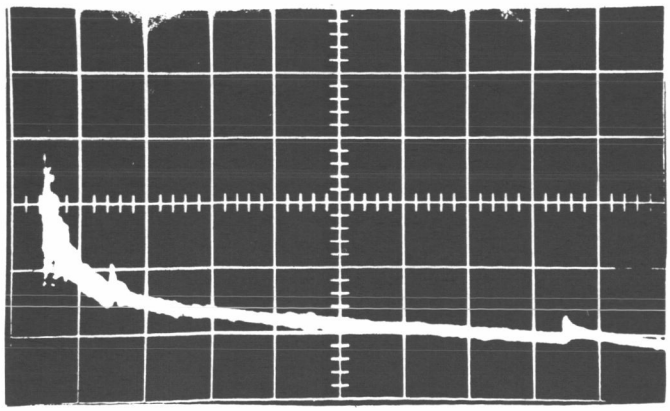

c

PLATE 13 Comparison of theoretical and experimental pressure histories (Position 6, vertical 50 psi/cm, horizontal 1 msec/cm)

a. Theory for inviscid and adiabatic flow
b. Theory including friction and heat transfer
c. Experimental result

a

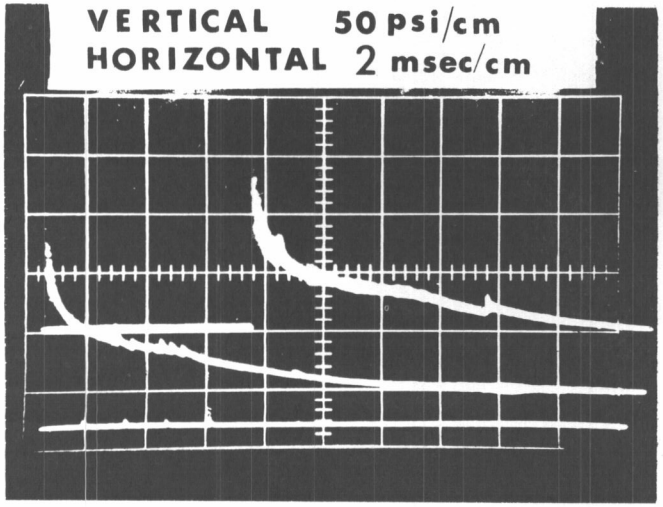

b

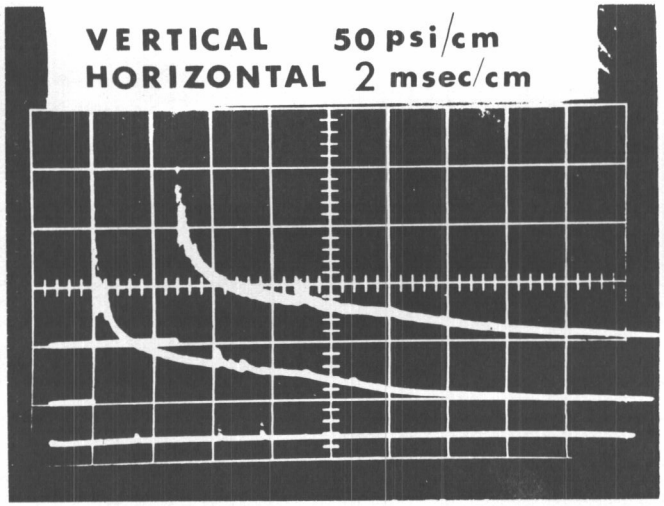

c

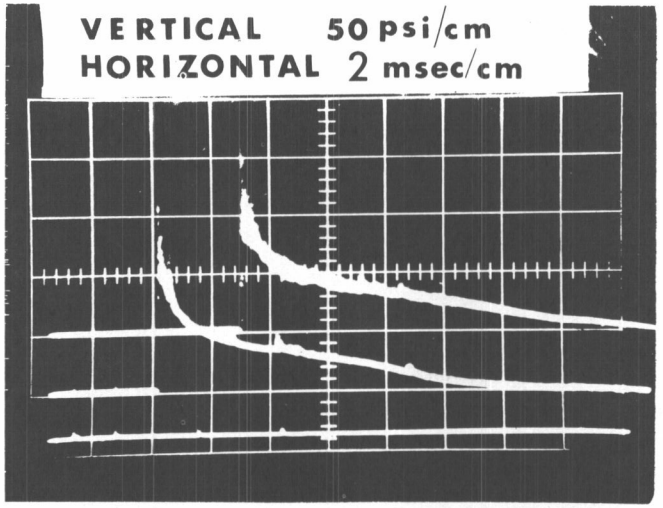

PLATE 14 Pressure histories at various positions along the tube wall
(Mixture: 40% H_2, 70% Air, at 70°F and 1 atm.)

a. Positions 1 and 6
b. Positions 2 and 4
c. Positions 3 and 5